



HAL
open science

Enhanced reactivity of copper complex-based reactive materials via mechanical milling

Tao Wu, Florent Sevely, Sylvain Pelloquin, Sandrine Assié-Souleille, Alain Estève, Carole Rossi

► **To cite this version:**

Tao Wu, Florent Sevely, Sylvain Pelloquin, Sandrine Assié-Souleille, Alain Estève, et al.. Enhanced reactivity of copper complex-based reactive materials via mechanical milling. *Combustion and Flame*, 2021, 233, pp.111598. 10.1016/j.combustflame.2021.111598 . hal-03312787

HAL Id: hal-03312787

<https://laas.hal.science/hal-03312787v1>

Submitted on 2 Aug 2021

HAL is a multi-disciplinary open access archive for the deposit and dissemination of scientific research documents, whether they are published or not. The documents may come from teaching and research institutions in France or abroad, or from public or private research centers.

L'archive ouverte pluridisciplinaire **HAL**, est destinée au dépôt et à la diffusion de documents scientifiques de niveau recherche, publiés ou non, émanant des établissements d'enseignement et de recherche français ou étrangers, des laboratoires publics ou privés.

Enhanced Reactivity of Copper Complex-Based Reactive Materials *via* Mechanical Milling

Tao Wu, Florent Sevely, Sylvain Pelloquin, Sandrine Assié-Souleille, Alain Estève, and Carole Rossi*

LAAS-CNRS, University of Toulouse, 7 Avenue du colonel Roche, 31400 Toulouse, France

Abstract

A prior investigation by the authors demonstrated that incorporating 25% of copper complex ($\text{Cu}(\text{NH}_3)_4(\text{NO}_3)_2$) into Al/CuO nanothermite enables to produce highly-reactive gas-generating energetic composites for emerging micro-airbag applications. To further improve the decomposition of the copper complex into gaseous species (N_2 , O_2 , N_2O), during the thermite reaction, we employed ball milling technique to diminish its grain size down to the nanoscale. Results show that premilling the copper complex *i.e.* refining its grains without much modifying their structures, increases the pressure generation and burn rate by a factor 1.5 and 2, respectively. It also maintains a high degree of performances along a wider range of thermite to copper complex mass ratio.

1. Introduction

Ball milling is a well-established, inexpensive and scalable technique for fabrication of different powdered materials [1,2]. For energetic materials including metastable alloys, Al/oxides reactive materials (RMs), ball milling technique allows their reactive properties to be enhanced through nano-structuring of the material [1,3]. Indeed, the strong mechanical stresses appearing in the course of ball milling usually leads to a reduction of the grains sizes down to nanometric sizes, typically on the scale of 100 nm, as well as an increase of the volume of the fraction of boundary regions [1,4], which define the kinetics of material ignition [1,5–7]. Here, it is applied here to tune the size of copper complex, $\text{Cu}(\text{NH}_3)_4(\text{NO}_3)_2$ (referred as to CuC), mixed with Al/CuO nanothermites to enhance the reactivity of the resulting gas generating material [8]. As synthesized, CuC particles contain large amount of big ($\sim 30 \mu\text{m}$) and non-uniform particles provoking inhomogeneous mixing with Al and CuO components and deficient thermal transfer within the composite; thus, penalizing burn rate and gas production yield. We present in this communication the effect of milling process on the resulting internal microstructures of the milled CuC powder and combustion behavior. The results show that premilling CuC improves both the RMs preparation, usability range and reactive properties.

2. Experimental

CuC was synthesized according to literature [8]. The as-synthesized CuC (raw CuC) were milled using a Retsch CryoMill machine with alumina grinding balls (diameter: 25 mm). In each milling vial, raw materials and grinding balls occupy 1/3 of the vial volume, respectively, leaving the rest 1/3 volume with air. This volumetric ratio was used under the instruction of the milling machine. Milling parameters: 30 Hz (30/s) for various duration (3, 10 and 20 min) with liquid N_2 cooling. The milled powder (labelled as $\text{CuC}^{\text{milled_milling time}}$) was then collected and stored in vials. The other experimental details are provided in supplemental file.

3. Results and Discussion

Figure 1a shows the X-ray diffraction (XRD) patterns of raw and milled CuC powders. It is observed that ball milling does not change its phase as the majority of the XRD peaks from

* Corresponding author.

E-mail address: rossi@laas.fr (Dr. C. Rossi)

both samples are aligned very well with the standard pattern of $\text{Cu}(\text{NH}_3)_4(\text{NO}_3)_2$ (PDF#01-070-0195). The XRD patterns of milled CuC remain unchanged for various milling times. Some variations in peak intensities of these two XRD patterns are noticed (Figure 1a), such as (141) vs (240), (040) vs (101), (301) vs (321), etc. After comparison, it appears that the XRD pattern of milled CuC resembles the reference pattern more than the raw CuC, which is likely affected by preferred orientation in raw CuC [9]. Preferred orientation is a measurement artifact caused by sample preparation and appeared more common in samples with distinct shape, such as the rod-shaped raw CuC (Figure S2), whereas milled CuC no longer features such shape but rather exhibits arbitrary morphologies. All in all, the milled CuC crystallites are more randomly oriented in the XRD experiment and therefore resembles the reference pattern more [9].

Peak broadening is spotted on peaks below 2θ 40° in the pattern of milled samples (Table S1), which might suggest smaller crystallite sizes are formed upon milling [10,11]. The average crystallite size extracted from the broadening of all peak widths labeled in Figure 1a using the Scherrer equation is about 49 nm for milled powder, versus 56 nm for raw ones [12,13]. Obviously, the milling does not pose much effect on reducing the crystallite size; but, importantly, it does affect the particle size significantly.

Figure 1b-j shows the SEM images of the three milled CuC. Indeed, the particle sizes of these milled samples decreased significantly (spanning from 1 to 10 μm) after milling comparing with the raw CuC rod-shaped particles (~ 20 μm in width and ~ 60 μm in length, see SEM images in Figure S2). It is clearly shown that the milled CuC particles feature no longer the rod-looking shapes but rather irregular profiles within micro-sized ranges. As observed in Figure 1b/1e/1h, there are still some particles larger than 5 μm remain existence after 3 minutes milling; when the milling is prolonged to 10 and 20 minutes, the CuC particles' size is mostly around 1 μm . In other words, longer milling time gives smaller particles size. In addition to reducing particles sizes, mechanical milling also develops more textures in micro/nano-scales (Figure 1f-g and 1i-j) on the surface of CuC milled for longer than 10 minutes when comparing to the smooth surface morphology of raw CuC rods. Such detailed textures could be resulted from fracturing/cracking of CuC particles induced by mechanical milling. The richness of the surface texture could potentially increase its surface area to promote a better contact with other components in the RMs. In fact, the corresponding BET measurements demonstrates an increase in the specific surface area of CuC powders after milling, ~ 0.7 m^2/g for raw CuC to ~ 3 m^2/g for CuC milled by 3 minutes.

The temporal pressure records of different CuC/Al/CuO RMs are presented in Figure S3. The pressure developed by Al/CuO thermite is included for the purpose of literature comparisons. Pressure peak values normalized per unit mass of the burnt materials are compared for different milling times in Figure 1k. The effect of milling is clearly established: regarding the maximum pressure, CuC-containing RMs with milled CuC outperform those with raw CuO by $\sim 45\%$. $\text{CuC}^{\text{milled}_{3\text{min}}}/\text{Al}/\text{CuO}$ features the highest increase ($\sim 52\%$) while the difference among all three milled composites can be neglected if we consider the experimental deviations. For pressurization rate, the trend is quite similar to the maximum pressure results, except $\text{CuC}^{\text{milled}_{10\text{min}}}/\text{Al}/\text{CuO}$ gives the fastest rate. But, again, the influence of the milling time is quite negligible.

Burning rate experiments, reported in Figure 1l and Video S1, give a similar trend. $\text{CuC}^{\text{milled}_{10\text{min}}}/\text{Al}/\text{CuO}$ features the highest velocity: 150 m/s against 85 m/s from CuC/Al/CuO (roughly 80% improvement) and 50 m/s for Al/CuO thermite system. $\text{CuC}^{\text{milled}_{3\text{min}}}/\text{Al}/\text{CuO}$ shows the smallest enhancement on propagation speed, possibly because the particles sizes of $\text{CuC}^{\text{milled}_{3\text{min}}}$ are larger than the other two milled powders. Note that the optimal milling time, 10 min, for burning rate follows that of the pressurization rate rather than the maximum

pressure. In fact, there is not much difference between the propagation speeds of $\text{CuC}^{\text{milled}_{10\text{min}}}/\text{Al}/\text{CuO}$ and $\text{CuC}^{\text{milled}_{20\text{min}}}/\text{Al}/\text{CuO}$; with the uncertainty bars, it seems that a longer milling time than 10 minutes does not further improve the propagation speed significantly.

Moreover, as we recall that Al/CuO to CuC mass ratio highly affects the self-combustion capabilities of CuC/Al/CuO RMs [8]. We found that the optimized weight percentage (wt%) of Al/CuO allowing a self-sustained decomposition of CuC, faster burn rate and maximum enhancement on peak pressure was 75%. For Al/CuO_{wt%} belows 75%, the CuC/Al/CuO combustion properties rapidly declines. When Al/CuO_{wt%} drops to 50%, the flame propagation was measured at 3 m/s and the flame quenches when Al/CuO_{wt%} reaches 25%: not enough thermite is in the system to sustain the CuC heating to its decomposition temperature (260 °C). In our previous article, the reaction mechanism of CuC/Al/CuO was detailed: Al/CuO ignites locally and the generated heat promotes decomposition of CuC; then the decomposition products of CuC further participate in Al/CuO thermite reaction [8]. Not only behaving as a gas generator, CuC also acts as the heat transfer medium within the RMs. Since CuC has a thermal conductivity lower than Al/CuO thermite, it could potentially act as hot points in the composite to increase local temperatures and enhance the overall reactivity, similar to the previous published works on the positive effects of silica/gold additions in RMs [14,15].

Thus, premilling CuC offers opportunity to take advantage of the spreading of smaller and denser hot points within the composite that empower it with a higher capability to rise in temperature. This is particularly visible for Al/CuO_{wt%} 50%: while this corresponds to a propagation limit at 3 m/s for CuC/Al/CuO using raw CuC, CuC/Al/CuO with premilled CuC (10 min) still propagate at a high velocity: 120 m/s (**Video S2**), which represents a gain of two order of magnitudes in the burn rate. Only decreasing CuC particles sizes, the propagation of CuC/Al/CuO improved extraordinarily due to the following two factors: 1) the thermal transfer between CuC and Al/CuO thermite is considerably improved after milling; 2) more CuC hot spots are spread within the RMs. Both factors facilitate the decomposition of CuC and heat transfer efficiency, thus accelerate the flame propagation.

Then, decreasing Al/CuO_{wt%} down to 25% still leads to quenching of the reaction as in the case of CuC/Al/CuO RMs prepared with raw CuC. This was expected as reducing the size of grains down to the nanoscale does not modify the thermal energy necessary to heat up the material to its decomposition temperature.

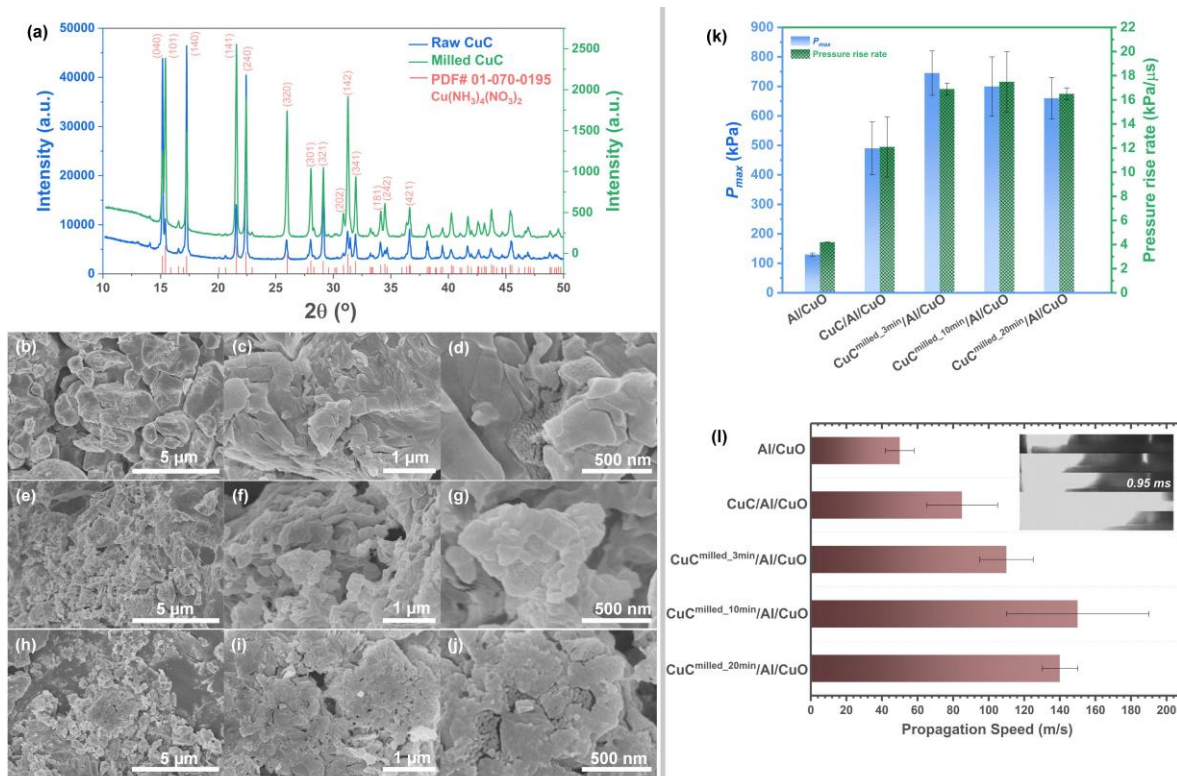


Figure 1. (a) XRD patterns of milled CuC in comparison to raw CuC; SEM images of CuC milled by 3 (b-d), 10 (e-g), and 20 minutes (h-j); maximum generated pressure and pressure rise rate (k), and propagation speed results (l) of different CuC/Al/CuO RMs. The inset image in (l) is a snapshot from the propagation test videos of these five materials at 0.95 ms (see supplement, **Video S1**).

Competing financial interests

None.

Acknowledgements

The authors acknowledge support from the European Research Council (H2020 Excellent Science) Researcher Award (grant 832889 – PyroSafe) and the Occitanie Region / European Union for their FEDER support (THERMIE grant). This work was also supported by LAAS-CNRS technology platform, a member of Renatech network. We acknowledge the help from Christophe Tenaillieu and Marie-Claire Barthélémy from CIRIMAT for performing XRD and BET measurements.

Supplementary materials

Supplementary materials associated with this article are available in a separate document.

References

- [1] C. Badiola, M. Schoenitz, X. Zhu, E.L. Dreizin, Nanocomposite thermite powders prepared by cryomilling, *J. Alloys Compd.* 488 (2009) 386–391. <https://doi.org/10.1016/j.jallcom.2009.08.146>.
- [2] C. Woodruff, E.R. Wainwright, S. Bhattacharia, S.V. Lakshman, T.P. Weihs, M.L. Pantoya, Thermite reactivity with ball milled aluminum-zirconium fuel particles, *Combust. Flame.* 211 (2020) 195–201. <https://doi.org/10.1016/j.combustflame.2019.09.028>.

- [3] M. Schoenitz, T.S. Ward, E.L. Dreizin, Fully dense nano-composite energetic powders prepared by arrested reactive milling, *Proc. Combust. Inst.* 30 (2005) 2071–2078. <https://doi.org/10.1016/j.proci.2004.08.134>.
- [4] H. Wang, J.B. DeLisio, T. Wu, X. Wang, M.R. Zachariah, One-step solvent-free mechanochemical synthesis of metal iodate fine powders, *Powder Technol.* 324 (2018) 62–68. <https://doi.org/10.1016/j.powtec.2017.10.024>.
- [5] S.M. Umbrajkar, S. Seshadri, M. Schoenitz, V.K. Hoffmann, E.L. Dreizin, Aluminum-Rich Al-MoO₃ Nanocomposite Powders Prepared by Arrested Reactive Milling, *J. Propuls. Power.* 24 (2008) 192–198. <https://doi.org/10.2514/1.31762>.
- [6] M. Schoenitz, T. Ward, E.L. Dreizin, Preparation of Energetic Metastable Nano-Composite Materials by Arrested Reactive Milling, *MRS Online Proc. Libr.* 800 (2003) 103–108. <https://doi.org/10.1557/PROC-800-AA2.6>.
- [7] E.L. Dreizin, M. Schoenitz, Mechanochemically prepared reactive and energetic materials: a review, *J. Mater. Sci.* 52 (2017) 11789–11809. <https://doi.org/10.1007/s10853-017-0912-1>.
- [8] T. Wu, F. Sevely, B. Julien, F. Sodre, J. Cure, C. Tenailleau, A. Esteve, C. Rossi, New coordination complexes-based gas-generating energetic composites, *Combust. Flame.* 219 (2020) 478–487. <https://doi.org/10.1016/j.combustflame.2020.05.022>.
- [9] J.K. Cockcroft, A.C. Jupe, Preferred Orientation, *Adv. Certif. Powder Diffr. Web.* (1997). <http://pd.chem.ucl.ac.uk/pdnn/pdindex.htm>.
- [10] T. Ungár, Microstructural parameters from X-ray diffraction peak broadening, *Viewp. Set No 35 Met. Alloys Struct. Scale Micrometer At. Dimens.* 51 (2004) 777–781. <https://doi.org/10.1016/j.scriptamat.2004.05.007>.
- [11] R. Yogamalar, R. Srinivasan, A. Vinu, K. Ariga, A.C. Bose, X-ray peak broadening analysis in ZnO nanoparticles, *Solid State Commun.* 149 (2009) 1919–1923. <https://doi.org/10.1016/j.ssc.2009.07.043>.
- [12] T. Wu, P.Y. Zavalij, M.R. Zachariah, Crystal structure of a new polymorph of iodic acid, δ -HIO₃, from powder diffraction, *Powder Diffr.* 32 (2017) 261–264. <https://doi.org/10.1017/S0885715617000859>.
- [13] V. Uvarov, I. Popov, Metrological characterization of X-ray diffraction methods for determination of crystallite size in nano-scale materials, *Mater. Charact.* 58 (2007) 883–891. <https://doi.org/10.1016/j.matchar.2006.09.002>.
- [14] H. Wang, J.B. DeLisio, S. Holdren, T. Wu, Y. Yang, J. Hu, M.R. Zachariah, Mesoporous Silica Spheres Incorporated Aluminum/Poly (Vinylidene Fluoride) for Enhanced Burning Propellants, *Adv. Eng. Mater.* 20 (2018) 1700547. <https://doi.org/10.1002/adem.201700547>.
- [15] B. Julien, J. Cure, L. Salvagnac, C. Josse, A. Esteve, C. Rossi, Integration of Gold Nanoparticles to Modulate the Ignitability of Nanothermite Films, *ACS Appl. Nano Mater.* 3 (2020) 2562–2572. <https://doi.org/10.1021/acsnm.9b02619>.